Using a hazard-independent approach to understand road-network robustness to multiple disruption scenarios

Philippe Y.R. Sohouenou [a,b,c,*], Luis A.C. Neves [a], Aris Christodoulou [c], Panayotis Christidis [c], Davide Lo Presti [b,d]

[a] Resilience Engineering Research Group, Faculty of Engineering, The University of Nottingham, Nottingham, UK
[b] Nottingham Transportation Engineering Centre, Faculty of Engineering, The University of Nottingham, Nottingham, UK
[c] European Commission, Joint Research Centre (JRC), Seville, Spain
[d] Department of Civil, Environmental, Aerospace, Materials Engineering, University of Palermo, Palermo, Italy

A B S T R A C T

A range of predictable and unpredictable events can cause road perturbations, disrupting traffic flows and more generally the functioning of society. To manage this threat, stakeholders need to understand the potential impact of a multitude of predictable and unpredictable events. The present paper adopts a hazard-independent approach to assess the robustness (ability to maintain functionality despite disturbances) of the Sioux Falls network to all possible disruptions. This approach allows understanding the impact of a wide range of disruptive events, including random, localised, and targeted link failures. The paper also investigates the predictability of the link combinations whose failure would lead to the highest impacts on the network performance, as well as, the correlation between the link-criticality rankings derived when only single-link failures are considered as opposed to when multiple-link failures are considered. Finally, the sensitivity of the robustness-assessment results to the intensity and distribution of the travel demand is evaluated.

1. Introduction

1.1. The need to consider multiple predictable and unpredictable disruptive events

Roads are essential to our increasingly connected urban systems as they support people's daily mobility, the freight industry, but also emergency services. Hence, natural and man-made hazards disrupting traffic flows threaten the functioning of society. To manage this threat, stakeholders need frameworks to assess and understand the potential impacts of a range of predictable and unpredictable events, and compare preparedness and response strategies.

So far, the dominant approach used to inform the management of disruptive events in engineering systems has been risk analysis, which typically involves three stages: risk identification and characterisation, risk exposure analysis, and consequences analysis. However, Park et al. (2013) challenge the applicability of risk analyses to complex systems (such as transport networks) that result from a dynamic interaction between engineering, human, and natural systems as several hazards occurring in such systems are unknown and unpredictable. To overcome this limitation, addressing the resilience (ability to sustain, resist, and recover from shocks) of

---

* Corresponding author.
  E-mail address: philippe.sohouenou@nottingham.ac.uk (P.Y.R. Sohouenou).

complex systems can be a more suitable approach since it is a dynamic property emerging and observable across a variety of disruption scenarios (Park et al., 2013). In other words, resilience analyses accept the possibility that a wide range of disruptive events may occur but are not necessarily predictable, and focus on anticipating and protecting the performance of the disrupted system rather than preventing or mitigating the loss of assets due to specific events (ARUP, 2014).

The present paper focuses on the robustness of road networks that is the ability to absorb perturbations. As the main function of road networks is to provide mobility (that is the ability to travel between trip origins and destinations in a timely manner) road networks' robustness should characterise their ability to deliver this function under a multitude of potentially unpredictable conditions. However, assessments of the potential impact of disruptive events on road networks generally focus on a limited set of scenarios illustrating the proposed methodology (Nogal et al., 2016; Omer et al., 2013; Zhang and Wang, 2016) or the worst-case scenario using a game theory approach (Alderson et al., 2017; Bhavathrathan and Patil, 2018; Bhavathrathan and Patil, 2015). These studies do not uncover the potential impact of all possible disruption scenarios as suggested by the resilience paradigm. This is unfortunate as such findings could be useful to practitioners and public authorities. For example, considering that a wide range of events (e.g. pavement maintenance, road accidents, flooding, etc.) can unpredictably disrupt any part of the network, the identification of multiple worst-case scenarios rather than the single worst-case scenario would be more useful in practice.

1.2. Research addressing multiple disruptive events

A range of recent studies consider multiple disruption scenarios in the road transport context. For example, Zhou et al. (2017) and Wisetjindawat et al. (2017) proposed interesting frameworks to consider multiple hazards. Both studies, however, belong to the risk analysis paradigm, which relies on records of past disruptions (including road accidents, maintenance and disasters), that may overlook unpredictable events as explained above.

Buhl et al. (2006), Sohouenou et al. (2020) and Casali and Heinimann (2020) performed hundreds to thousands of realisations of different types of dismantling processes on self-organised street networks (e.g. Rome), artificial and real road networks, and the Zurich road network, respectively. Dismantling processes that progressively remove nodes (or links) from the network are often used in complex network theory to understand how many nodes (or links) must be removed to fragment a network into isolated components. Robustness is then measured by the change of some metric of the network functionality against the fraction of removed nodes. These studies present two practical drawbacks. The first drawback is linked to the transport modelling approach. This approach analyses the network topology (the arrangement of the roads and intersections) but disregards traffic flows and capacity constraints. Hence, this approach is unable to capture dynamic effects of the disruption such as increased congestion on alternative routes and the related behavioural responses (Mattsson and Jenelius, 2015).

The second drawback is that only full dismantling processes are considered to model disruptive events. Dismantling process analyses are useful to determine the critical number of failed components after which networks can no longer function. This information is important, for example, to address mutations and router problems in gene and computer networks respectively (Reka et al., 2000). For road networks, this information is relevant only when analysing major disasters (e.g. earthquakes or large floods) that can potentially damage many roads. This is because contrary to computer or social networks, road networks are composed of large physical infrastructures that are difficult to damage. Hence, dismantling processes lack applicability to a wide range of road perturbations such as car accidents, sabotage actions and landslides that disrupt a limited number of roads. Besides, experience showed that the unavailability of a small fraction of a transport network can lead to major consequences for society and the economy. For instance, the collapse of the I-35 W Bridge in Minneapolis (USA) resulted in economic losses of US$71,000 to US$220,000 a day (Xie and Levinson, 2011). Hence, a better understanding of the potential impacts of events disrupting a limited number of links and intersections remain important in practice. Noting this, Sohouenou et al. (2020) also consider disruption scenarios concurrently affecting one to three links to determine the relationship between network robustness, network size and damage extension (number of failed links).

Robustness studies based on traffic flow modelling, which consider travel demand and capacity constraints, generally provide a more realistic assessment of the consequences of disruptions for the users and society (Mattsson and Jenelius, 2015). However, in comparison to topological analyses, traffic flow analyses present two major disadvantages: their data hungriness and computational complexity. These analyses require travel demand data and calibrated behavioural models that are often unavailable. Besides, considering the computational effort required for traffic simulations, it is currently unrealistic to perform thousands of disruption simulations that each require a traffic analysis as with topological analyses. This is especially true for large networks as the computational effort of traffic simulations exponentially increases with the network size. Ganin et al. (2017) performed twenty realisations of disruption scenarios affecting a random and finite number of links on traffic flow models of 40 US cities. For the sake of computational effectiveness, the authors removed residential streets and service roads as well as intersections with only one and two links from their analysis. Ganin et al. (2017) show that this removal has an insignificant effect on estimated speeds and numbers of lanes. The purpose of the study was to compare efficiency (annual delay in peak-periods under normal conditions) and resilience (annual delay in peak-periods due to disruption) across different network topologies. Hence, the impacts of the different disruption scenarios were not studied in detail and the number of scenarios considered relatively limited.

In contrast, a certain group of studies, that can be called link criticality studies, traditionally consider a full range of predictable and unpredictable disruption scenarios. These studies seek to identify the links whose failure would result in the highest impacts on the network performance. The rationale for such studies is that the most critical roads should be given top priority for pre-event reinforcement and post-event restoration. To identify critical links in a network, Taylor et al. (2006) proposed an approach based on single-link failures (SLFs) where each link is removed from the network and the corresponding effect on the network performance is estimated. The levels of impact are then ranked and the links demonstrating the most significant impacts are considered the most critical.

This approach has been widely adopted and improved in subsequent studies (Omer et al., 2013; Sullivan et al., 2010) that also considered link capacity reductions rather than complete link removal. However, capacity reductions add to the already high computational cost of this approach since several scenarios need to be computed per link.

A growing concern in link criticality studies is that this approach disregards the effect of multiple-link disruptions. Wang et al. (2016) showed that the most critical links in multiple-link failures (MLFs) are not simply the combination of those resulting from the most critical single-link failure. Hence, the consideration of single-link failures only is insufficient as this approach could lead to inefficient prevention and restoration measures in the advent of events disrupting several road segments or several events concurrently affecting different parts of the network. Sohouenou et al. (2020) showed that in road networks the correlation between the link criticality rankings based on SLFs and MLFs was controlled by the proportion of nodes being OD points while other parameters including the network size, the network topology, and the heterogeneity of the link travel costs in the network did not influence the rankings correlation. However, that study was topological and therefore did not consider capacity constraints and potential congestion.

Ultimately, although research has extensively contributed to the understanding of road network robustness, characterisation of the potential impacts of a full range of predictable and unpredictable disruption scenarios in congested networks is still lacking. To increase this understanding, the present paper uses a traffic model to assess the robustness of the Sioux Falls network to multiple disruption scenarios. The Sioux Falls network is studied for two reasons. The first reason is computational effectiveness. This network model is composed of only 24 nodes and 76 directed links, which lead to reasonable traffic-simulation run times (under five seconds). This short run time allowed the performance of over five hundred thousand disruption simulations using parallel processing on a normal computer. The second reason is reproducibility. The Sioux Falls network dataset is readily available, for example on the Transportation Networks for Research repository (Transportation Networks for Research Core Team, 2019), and has been extensively used in the transport literature (Bhavathrathan and Patil, 2015; Mitradjieva and Lindberg, 2013; Wang et al., 2016).

1.3. Scope, purpose and structure of the study

As stated above, the present paper focuses on the robustness of road networks that is the ability to absorb perturbations. The purpose of the study is to evaluate how the availability of alternate routes and capacity helps remediate the consequences of initial disruptions to the network. These consequences mainly depend on the network topology, capacity and travel demand, and on the disruption type, extension and impacts on the system performance, which are all considered. The immediate response (in terms of closing lanes or reducing speed limits on affected roads) and the speed of restoring full functionality (through repair actions) are considered outside the scope of this study although it is noted that they would be required to fully capture the resilience of a transport system.

To assess the robustness of the Sioux Falls network, this paper develops and uses a set of meaningful robustness indicators suitable to discriminate between the impacts of a wide range of disruptive events, as well as, a method to identify the most critical links in a network using multiple-link failures. The study adopts a hazard-independent approach in line with the resilience paradigm, where all scenarios disrupting multiple links (more specifically up to five links) are considered. The study focuses on disruption scenarios concurrently affecting up to five-undirected links for computational effectiveness. It was assumed that single- to five-link failures could provide enough data points to understand the effect of the damage extension (number of disrupted links) on the Sioux Falls network. This seems true as certain two-link failures already fragmented the Sioux Falls network model and certain five-link failures (that disrupt 13% of the undirected links in the Sioux Falls network) caused 87% decreases in performance, measured by travel time increases.

The hazard-independent approach allows the comparison of the impacts of three types of damage, namely, random (damaging random sets of links), localised (damaging adjacent links), and targeted (seeking to maximise the damage to the system performance). The robustness analysis of the Sioux Falls network is also used to explore the predictability of the link combinations whose failure would lead to the highest impacts on the system performance, and the difference between of the link criticality rankings (identifying the links whose failure would result in the highest impacts on the system performance) when only SLFs are considered as opposed to MLFs. Finally, the effects of demand intensity and distribution variability (and therefore congestion) on the network robustness and link criticality metrics are assessed to provide a clearer understanding of road network robustness dependency on travel demand conditions.

The paper is structured as follows. Section 2 presents the methods and case study. In Sections 3 and 4, the results of the network robustness assessment are presented and discussed, respectively. Sections 5 provides some concluding remarks.

2. Methods

2.1. Disruption model

Disruptive events can impact both the supply and the demand side of the transport system. The supply side (i.e. the network) is affected by the damage induced on the infrastructures, which in turn impacts traffic conditions through road unavailability as well as speed and capacity reductions. The demand side representing the flow of users can also be impacted as trips may be cancelled or delayed due to usual routes and destinations being affected. As this study seeks to evaluate how the availability of alternate routes and capacity helps remediate the consequences of network disruptions, travel demand was considered fixed to effectively compare the network performance under different disruption scenarios (all other things being equal).

As road disruptions are rarely predictable, the present paper adopted an "all-hazard" approach in line with the resilience paradigm. All possible combinations of link failures disrupting up to five links at the same time were simulated. This resulted in a dataset that combined five levels of damage extension: single-, two-, three-, four- and five-link failures.

The disruption scenarios in this dataset were then categorized into three types of disruptions, that are, localised-, targeted-, and random- link failures. Localised scenarios disrupt adjacent links. These scenarios can be identified using the following procedure:

1. Identification of all localised two-link combinations
   (i) for each link, a_1, in the network, search for all links, $a_2 \neq a_1$, adjacent to a_1 (i.e. connected to the same node) and store (a_1, a_2) in a dataset
   (ii) remove duplicates from the dataset
2. Identification of all localised three-link combinations
   (i) for each link combination, (a_1, a_2), search for all links, $a_3 \neq a_1 \& a_2$, adjacent to a_1 and for all links, $a_3 \neq a_1 \& a_2$, adjacent to a_2, and store (a_1, a_2, a_3) in a dataset
   (ii) remove duplicates from the dataset
3. Identification of all localised four- and five-link combinations
   (i) repeat step 2 using the localised three- and four-link combination datasets, respectively

It is noted that localised disruptions are normally specified in terms of hazard-prone areas derived from climate models (Casali and Heinimann, 2019; Hu et al., 2016; Demirel et al., 2015; Wisetjindawat et al., 2017). In this paper, localised failures refer to a range of events that may differ in nature (flooding, landslide, or large demonstrations) but lead to similar consequences, that is, the unavailability of adjacent network components. Again, this approach is used to reduce the dependency of the robustness assessment on empirical data, which may overlook unpredictable events.

Unlike localised disruptions that lead to aggregated destruction of components in a limited area, targeted and random link failures can damage network components distributed throughout the whole system. The latter damage a random set of links (e.g. pavement maintenance, pipe bursting, or police incidents amongst others can lead to random road closures) whereas targeted attacks imply a driving force seeking to maximise damage to the network performance (e.g. the bombing of a critical bridge). Robustness studies – especially in the context of complex network theory – commonly distinguish between these two types of failures (Buhl et al., 2006; Reka et al., 2000; Zanin et al., 2018), while localised failures are increasingly considered (Hu et al., 2016).

In this study, targeted attacks correspond to the top 5% scenarios in each damage extension group (dataset) that cause the highest increases in travel time, measured by the network robustness indicator (presented below). The random failures correspond to the scenarios that are neither localised nor targeted.

Table 1 presents the definitions, models and real-world events associated with the three types of scenarios. The events presented in Table 1 could lead to partial speed or capacity reductions rather than complete road obstructions. However, the inclusion of such effects would add to the already high computational cost of the hazard-independent approach since several scenarios need to be computed per link.

2.2. Network robustness metrics

Robustness metrics should compare the required- and disrupted-network performance to evaluate the ability of the system to provide functionality despite disruptions. As the definition of the required performance is arbitrary (since it depends on the judgement of the transport operators, public authorises and users), the network pre-event performance is often used as a proxy for the required performance. Most robustness indices described in the literature consider the change in total travel time (TT) in the network (Bhavathrathan and Patil, 2015; Ganin et al., 2017; Omer et al., 2013). This metric is however unable to discriminate between scenarios leading to few or many Origin-Destination (OD) pair disconnections as these scenarios all lead to very high increases in total TT (Sohouenou et al., 2019). This is unfortunate as it is also useful in practice to discriminate between such scenarios since they lead to different proportions of stranded road users. Therefore, the present study adopts a novel robustness indicator able to differentiate between the impacts of scenarios leading to OD pairs disconnections. This indicator is an improvement to the standard indicators based on the total TT change. It is computed in two steps. Firstly, a travel time relative change index (TTC_w) is computed for each OD pairs:

Table 1
Classification and model of disruptive events affecting road networks.

Name	Definition	Model	Real-word events represented
Localised	Failure of adjacent links	Failures identified by the iterative procedure (above)	Flooding, Landslides, Large demonstrations
Targeted	Failure with a maximum impact on network performance	Failures leading to the top-5% lowest robustness indicator values	Targeted bombing, Sabotage, Industrial actions
Random	Failure of randomly selected links in the network	Failures that are neither critical nor localised	Serious car accidents, Road works, Police incidents

$$TTC_w = \left(1 + \frac{TT_d^w - TT_0^w}{TT_0^w}\right)^{-1} \tag{1}$$

where TT_0^w and TT_d^w are the undisrupted and disrupted travel times on the OD pair w, respectively. The travel time change index decreases as the travel time increases. TTC_w can take the value 1 if the TT remains equal to the initial travel time (TT_0^w) despite the disruption. TTC_w can also exceed 1 for OD pairs whose road users experience a decreased TT due to reduced congestion on some roads that they share with users who had to reroute due to the disruption.

The network robustness indicator (RO) then combines the TT change indices of all OD pairs using a weighted average:

$$RO = \sum_w k_w TTC_w \tag{2}$$

where w and k_w are an OD pair and the associated weighting factor, respectively. k_w is given by the ratio between the demand for w and the total demand in the network. As disruptions cause an increase in TT in most OD pairs, the network robustness indicator (RO) remains between 0 and 1. $RO = 100\%$ indicates that despite the disruptive event the TT remains roughly equal to the initial travel time on all OD pairs. Otherwise, the network robustness decreases as TT_d^w increases, the drop being more important when highly demanded routes are impacted.

To complement RO, several measures of the spread of the impacts across the OD pairs can be used. Among these measures, the most meaningful could be the proportion of road users unable to reach their chosen destination following the disruption. These users wish to travel between disconnected OD pairs whose TTC_w tend to zero (as the TT between the trip origin and destination becomes infinite). Hence, the proportion of users unable to reach their chosen destination – also called unsatisfied demand (USD) – is given by:

$$USD = \sum_w k_w \delta_w$$

$$\text{where } \delta_w = \begin{cases} 0, & \text{if } TTC_w < 0.001 \\ 1, & \text{otherwise} \end{cases} \tag{3}$$

For a more detailed assessment, the travel time in Eqs. (1)–(3) can be replaced by a generalised travel-cost metric considering other route choice factors such as distance, tolls, and scenery. The weighting factors (k_w) can also be adapted to give more importance to critical routes used by emergency services, for example.

To demonstrate the ability of RO to discriminate between a wider range of perturbation scenarios than total TT based indicators, the relative change of the total travel time ($ToTTC$) was also computed and compared with RO.

$$ToTTC = \left(1 + \frac{ToTT_d - ToTT_0}{ToTT_0}\right)^{-1} \tag{4}$$

where $ToTT_0$ and $ToTT_d$ are the undisrupted and disrupted total travel times, respectively. $ToTTC$ provides a measure of the change in system-wide travel time scaled in [0,1].

2.3. Link criticality assessment

2.3.1. Link criticality indicator

To identify the most critical links with regards to multiple-link failures, a criticality index was computed for each link depending on the impact of its unavailability on the network performance in all of the scenarios considered. The criticality index (Cr_a) of link a is:

$$Cr_a = \sum_s \frac{1}{L_s} \langle 1 - RO_z \rangle_s^a \tag{5}$$

where RO_z is the network robustness to hazard z (Eq. 2). s and L_s indicate a damage extension group (e.g. 2LFs) and the number of links damaged by the hazards of this group, respectively. The division by L_s means that failed links were assumed to equally contribute to the loss of performance. $\langle 1 - RO_z \rangle_s^a$ means that $1 - RO_z$ is averaged over the scenarios of the same size s in which a is damaged. The averages per scenario size ensure that the contributions of the different scenario sizes to the link criticality are in the same range. Indeed, there are more scenarios of multiple-link failures than SLFs. If L is the number of links in the network, there are one, $(L-1)$ and $(L-1)(L-2)$ scenarios of SLF, 2LFs and 3LFs per link, respectively, hence a simple sum would inherently give more importance to multiple-link failures. The criticality index of a non-critical link would tend to zero as the network robustness to the hazards involving the failure of this link will be close to 1, causing Cr_a to increase with the link criticality.

2.3.2. Comparison of the link criticality rankings derived from single- and multiple-link failures

As explained above, Wang et al. (2016) showed that the most critical links when multiple-link failures occur are not simply the combination of the most critical links with single-link failures. Still, as MLFs add to the computational cost of link-criticality studies, there is a need to understand whether SLFs can provide a reasonable approximation of the criticality rankings resulting from MLFs. Noting this, Sohouenou et al. (2020) quantified the difference between the link rankings based on single- and multiple-link failures,

and evaluated the sensitivity of this difference to several network characteristics using topological network representations. To complement that study, the present paper investigates the sensitivity of the difference between SLF- and MLF-based link criticality rankings to capacity constraints and travel demand variability.

To compare the rankings derived from MLFs (using Cr_a) with the rankings derived from SLFs, Spearman's rank-order correlation coefficient (R_S) was used. This coefficient provides a measure in [-1, 1], where -1 and 1 indicate a very strong negative and positive correlation respectively while zero indicates no correlation (Puth et al., 2015).

2.4. Case studies

2.4.1. The original Sioux Falls network

The present study analyses the robustness of the Sioux Falls (USA) network. Firstly introduced in LeBlanc et al. (1975), the Sioux Falls network (Fig. 1) has been extensively used as a case study in the literature (Bhavathrathan and Patil, 2018; Mitradjieva and Lindberg, 2013; Wang et al., 2016). This network consists of 24 nodes, 76 directed links, and 24 OD zones. The datasets describing this case study were obtained from the Transportation Networks for Research repository (Transportation Networks for Research Core Team, 2019). These datasets provide the network structure, link characteristics (including capacity, length, and free-flow travel time) and the origin-destination trip matrices.

2.4.2. Transport model

A standard transport model was used to compute and compare the travel time of road users in the initial and disrupted conditions. Using the demand matrix available at the Transportation Networks for Research repository (Transportation Networks for Research Core Team, 2019), traffic was assigned to the network assuming that users independently minimised their *TT*. Although individual driving habits may vary (D'Lima and Medda, 2015), this assumption seems reasonable in the absence of more detailed data as it was adopted in a traffic model validated against traffic data from 40 US urban areas (Ganin et al., 2017). This model is the fourth stage of the seminal four-step (trip generation, trip distribution, modal split, and traffic assignment) transport model (Ortuzar and Willusem, 2011) that can be used to estimate the number of vehicles (or people) that will use a specific transport facility based on travel data that can be obtained through census information, surveys, and estimates.

The travel time of link a (t_a) is defined by the standard BPR function (Bureau of Public Roads, 1964):

$$t_a(x_a) = t_a^f \left[1 + 0.15 \left(\frac{x_a}{c_a} \right)^4 \right] \qquad (6)$$

where x_a, c_a and t_a^f are the link flow, capacity and free-flow travel time, respectively.

The simulations were performed in Julia language (v.1.2) using the packages *Distributed*, *LightGraphs* and *TrafficAssignement* for
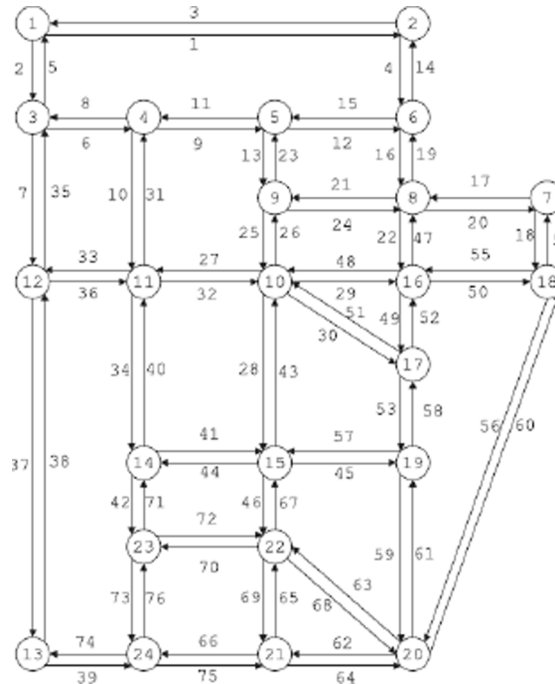

Fig. 1. Sioux Falls test network.

parallel processing, network analysis and traffic assignment computation, respectively. The latter implements three methods to find the user equilibrium: the original, conjugate, and bi-conjugate Frank-Wolfe (FW) algorithms (Mitradjieva and Lindberg, 2013). FW algorithm is one of the most popular methods used to solve traffic assignment problems while the conjugate and bi-conjugate versions of this algorithm improve its convergence speed. The fast bi-conjugate FW algorithm was used here with a relative convergence gap of 10^{-4}, which is a sufficient criterion for equilibrium stability (Boyce et al., 2004). To model link closures, a very high free-flow travel time (10,000 min) was assigned to unavailable links.

2.4.3. Evaluation of the effect of the demand distribution and level on the network robustness patterns

To provide a clearer understanding of road network robustness dependency on travel demand conditions, the effect of the demand intensity and distribution on the Sioux-Falls-network robustness and link criticality metrics was evaluated. In the original Sioux Falls network, the travel demand is heterogeneously distributed across all intersections as every node is both a trip origin and destination point (Fig. 2). To evaluate the effect of the demand distribution, two extreme cases were considered. Firstly, a case where the travel demand between all OD zones of the Sioux Falls network was removed from the network and homogeneously distributed among six arbitrarily chosen nodes: 1, 8, 10, 12, 20, and 23 (Fig. 1). Secondly, a case where the demand was homogeneously distributed to all nodes in the network was considered.

To evaluate the effect of the demand intensity, both extreme cases were computed under three levels of demand: low, medium, and high. The high level corresponds to the total demand in the original Sioux Falls network (360,600 vehicles/hour) that is already congested. The low (72,120 vehicles/hour) and medium (180,600 vehicles/hour) levels correspond to 20% and 50% of the total demand in the original network, respectively. These demand levels were chosen to obtain uncongested, congested, and highly congested case studies.

3. Results

The links of the Sioux Falls network (Fig. 1) were disrupted in both directions at the same time leading to 38 single-, 703 two-, 8436 three-, 73,815 four- and 501,942 five-link failures. Hence, the robustness and link criticality indicators measured the impact caused by the unavailability of both directions. For consistency, the link flows refer to the sum of the flows in both directions in this paper. However, as the demand in the Sioux Falls network is not totally symmetric a link might be more critical in one direction than the other. For the original Sioux Falls network, the simulations took 41 hours using parallel processing on an *Intel i3-7100* 3.9 GHz and 8 GB memory workstation.

3.1. Comparison of the network robustness indicators

The impacts of all possible single- to five-link failures on the Sioux Falls network were evaluated using the network robustness indicator, *RO* (Eq. 2), which measures the demand-weighted average increase in travel time along the OD pairs. The impacts were also evaluated using the total travel time change indicator, *ToTTC* (Eq. 4), which measures the relative change of the total travel time (often used as a robustness indicator in the literature). The results are shown in Fig. 3, where the values and kernel density of the network robustness indicator are compared to that of the total *TT* relative change indicator for the five damage extension groups. In Fig. 3.b, the unsatisfied demand indicator, *USD* (Eq. 3), is used to distinguish between the disruption scenarios that lead unsatisfied demand (grey points) and the scenarios that do not lead to unsatisfied demand (yellow points).

In Fig. 3.a, both indicators present single-peaked distributions, however, the distributions of the total TT change indicator have less pronounced peaks than the network-robustness-indicator distributions. Furthermore, it can be observed in Fig. 3.a that *ToTTC* progresses more quickly towards zero than *RO* as the damage extends. Some 2LF, 3LF, 4LF and 5LF scenarios have *ToTTC* values close to zero while their *RO* values remain superior to 0.475, 0.322, 0.223 and 0.126, respectively.
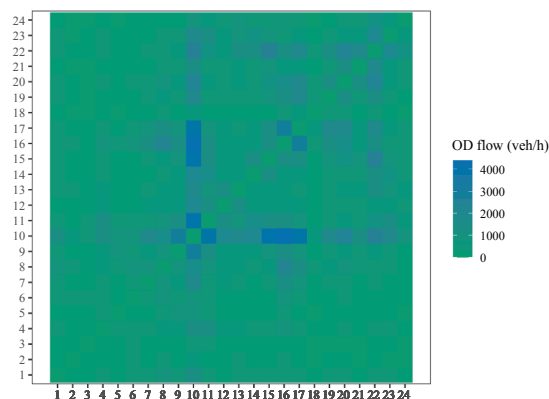

Fig. 2. Demand distribution in the original Sioux Falls network (OD = Origin-Destination).
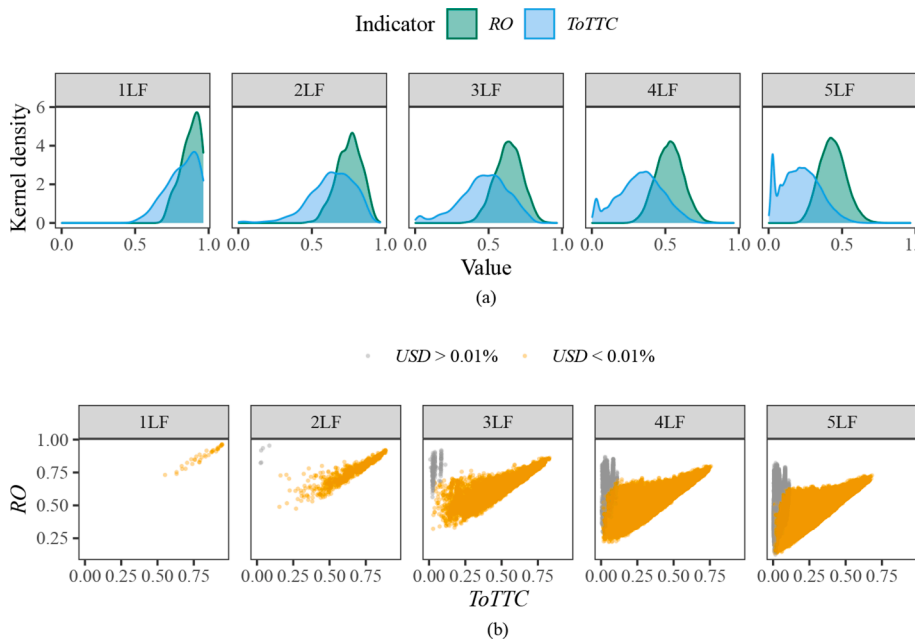
Fig. 3. Comparison of the network robustness (*RO*) and total travel time change (*ToTTC*) indicators under single- (1LF), two- (2LF), three- (3LF), four- (4LF) and five- (5LF) link failures in the original Sioux Falls network.

Three domains appear in Fig. 3.b regardless of the damage extension group. On the left side of the plots (*ToTTC*⩽0.10), *RO* is independent of *ToTTC* (vertical lines). On the right side (*ToTTC* > 0.5), the two indicators appear linearly correlated ($R^2 = 0.80$). Between these two domains, the linear model is less relevant ($R^2 = 0.42$).

The *ToTTC* values close to zero correspond to link combinations whose failure cause OD-pair disconnections measured by a non-zero *USD* value (grey points in Fig. 3.b). For example, the simultaneous disruption of (1,2) and (1,3) isolates node 1 from the rest of the
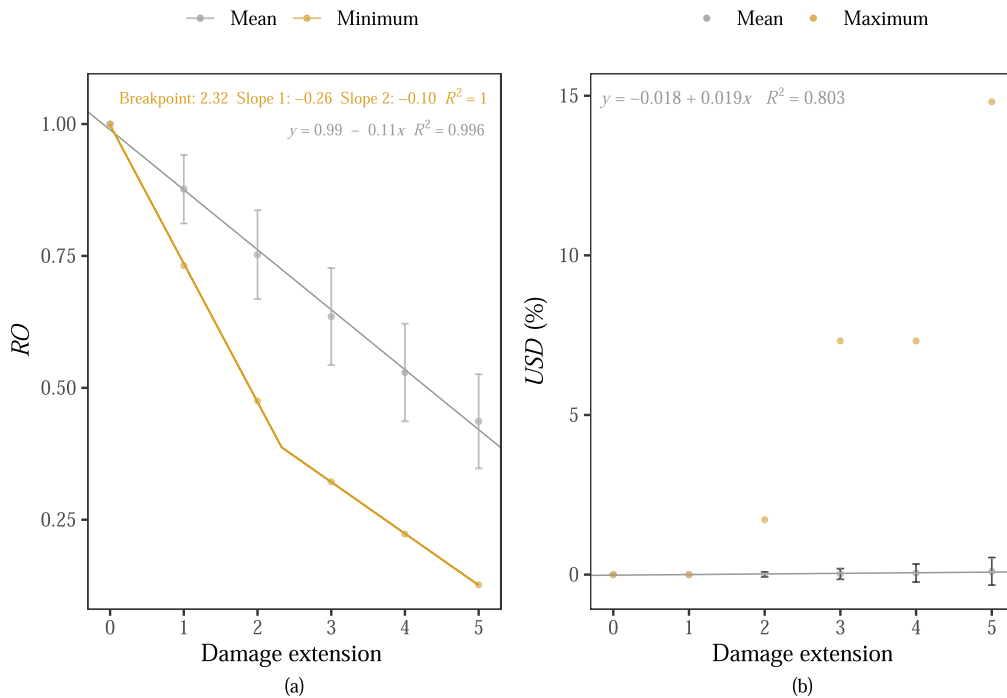

Fig. 4. Evolution of the network robustness (*RO*) and unsatisfied demand (*USD*) indicators depending on the damage extension (number of failed links) in the original Sioux Falls network. Error bar = mean ± sd.

network and disconnects all OD pairs involving this node as suggested by the network structure (Fig. 1). Besides, none of the 1LFs lead to OD pair disconnections, which explains why none of the 1LFs have a *ToTTC* value close to zero.

3.2. Evolution of the disruption impact depending on the damage type and extension

3.2.1. Extended impact of single- and multiple-link failures

The simulations considered five levels of damage extension (from single- to five-link failures) that had an increasing impact on the Sioux Falls network performance. Fig. 4 shows the evolution of the mean and minimum, and mean and maximum values of *RO* and *USD* across the damage extension groups, respectively.

In Fig. 4.a, the mean robustness indicator value quickly decreases as the damage extension increases (from 86.7% in 1LFs to 43.6% in 5LFs), while the standard deviation of *RO* remains steady (between 6.50% and 9.30%). A regression analysis showed that the relationship between the mean robustness indicator value and the damage extension could be captured by a linear model ($R^2 = 1$). The relationship between the minimum robustness indicator values and the damage extension could be captured by a piecewise linear model ($R^2 = 1$), where the minimum value of *RO* linearly decreases as the damage extension increases, the slope being sharper before the breakpoint (≈ 2.32). This breakpoint is close to two, which is the minimum number of links required to fragment the Sioux Falls network and cause unsatisfied demand (as shown in Fig. 4.b).

In Fig. 4.b, the mean *USD* value barely increases with the damage extension (from 0% in 1LFs to 0.1% in 5LFs), which shows that most scenarios do not disconnect the OD pairs. In comparison, the maximum value of *USD* increased in steps (from 0 in 1LFs and 2LFS to 1.7% in 2LFs to 7.3% in 3LFs and 4LFs, etc.). The standard deviation of *USD* increased with the damage extension, meaning that the heterogeneity of the potential impacts of the failure scenarios on the proportion of stranded users increased with the number of failed links.

3.2.2. Impact of localised, random and targeted link failures

Subsets of the 2LF, 3LF, 4LF and 5LF scenario sets were considered to assess the difference between the impacts of localised, targeted, and random damage using the disruption model described in Section 2.1. The impacts of the three types of scenarios are compared in Fig. 5. Fig. 5.a shows the relationship between the network robustness indicator measuring the average increase in *TT* along the OD pairs and the unsatisfied demand indicator measuring the proportion of road users unable to reach their chosen destination. Fig. 5.b and c show the distributions of *RO* and *USD* across the damage type and extension groups.

The results indicate that targeted attacks were much more critical to the network performance than random failures (the difference between the mean robustness to random and targeted failures being 19.4%, 20.3%, 19.5% and 17.9% in 2LFs, 3LFs, 4LFs and 5LFs, respectively in Fig. 5.b) while localised failures were only slightly more critical than their random counterparts (the difference between the mean robustness to random and localised failures being 1.6%, 2.9%, 4.0% and 4.3% in 2LFs, 3LFs, 4LFs, 5LFs respectively in Fig. 5. b). In addition, the difference between the mean robustness in localised and random failures increased with the damage extension while the difference between targeted and random failures seemed relatively constant.
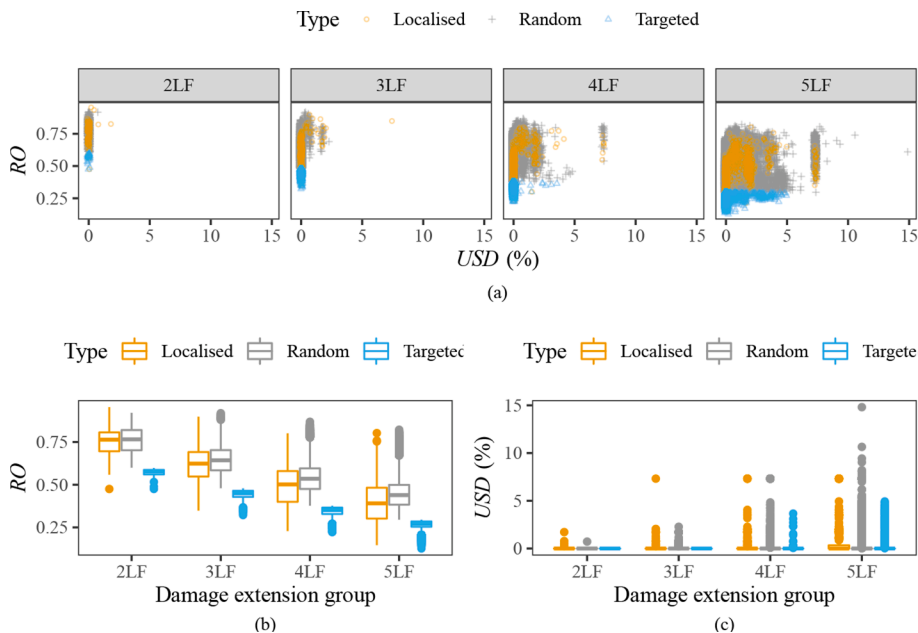

Fig. 5. Impact of localised, random and targeted two- (2LF), three- (3LF), four- (4LF) and five- (5LF) link failures in the original Sioux Falls network. (*RO* = Network robustness indicator, *USD* = Unsatisfied demand indicator, box = 25th and 75th percentiles).

Although the differences between the mean *USD* values in the three damage types were insignificant ($< 1.0\%$), it can be seen in Fig. 5.a and c that the highest values of the unsatisfied demand indicator appeared among the localised scenarios four all damage extension groups except 5LFs. In contrast, the targeted attacks presented the lowest *USD* values.

3.3. Most critical disruption scenarios

The network robustness indicator was used to identify the top-5 most critical scenarios in all damage extension groups. These scenarios are presented in Table 2 along with their *RO* and *USD* values. Table 2 excludes the most critical 5LF scenarios for the sake of brevity.

In accordance with the results presented in Fig. 5, it can be seen in Table 2 that none of the top-5 most critical scenarios led to unsatisfied demand (*USD* = 0). Besides, among the top-5 most critical scenarios only one was a localised scenario that is (9,10) & (10,11) in bold in Table 2.

The most critical combinations of 2LFs, 3LFs and 4LFs did not necessarily involve the most critical links with SLF as links outside of this group, for example (10,11) and (17,19), appeared in these combinations. However, all top-5 most critical 2LF scenarios involved the disruption of at least one of the top-6 most critical links with SLF, (5,9) being the 6th most critical link with SLF. Similarly, the top-5 most critical 3LFs and 4LFs all contained one of the top-5 most critical combinations of 2LFs and 3LFs, respectively. The critical combinations of 2LFs, 3LFs, and 4LFs hence involved at least one of the most critical links with SLF.

This pattern suggests that to identify and evaluate the impact of the top-5 most critical MLF scenarios it might not be necessary to consider all possible scenarios. Instead, an iterative procedure could be used as follows (in a network composed of L links):

(i) Evaluate the impact of all SLFs [L simulations]
(ii) Rank the impacts and select the top-10 most critical links (and not the top-5 to reduce the probability of missing critical scenarios)
(iii) Compute all 2LF scenarios involving the top-10 most critical links with SLF [$10(L-1)$ simulations]
(iv) Rank the impacts and select the top-10 most critical 2LFs
(v) Compute all 3LF scenarios involving the top-10 most critical 2LFs [$10(L-2)$ simulations]
(vi) Repeat the two previous steps until reaching the desired number of failed links

Therefore, to identify the top-5 most critical scenarios concurrently disrupting M links, this procedure would require $L + 10\sum_{k=1}^{M-1}(L-k)$ disruption simulations (1,118 in the Sioux Falls network for 4LFs), which is far less computationally expensive than the $\binom{L}{M}$ simulations required to test all possible scenarios (78,315 in the Sioux Falls network for 4LFs).

3.4. Critical links

As the most critical failure scenarios involve a multitude of links including links that are only critical when they concurrently fail with a specific set of other links (Table 2), it is difficult to rank links using the top-5 most critical scenarios only. Therefore, the link criticality was assessed using the link criticality indicator, Cr_a (Eq. 5), which combines the robustness indicator values of all single- and multiple-link failure scenarios into one indicator.

According to Cr_a, the most critical links in the Sioux Falls network were in criticality order, (10,15), (18,20), (9,10), (12,13), and (6,8), which is consistent with the SLF results (Table 2). To verify if the ranking provided by Cr_a was totally consistent with the SLF-based criticality rankings, the difference between the two rankings was evaluated using Spearman's correlation coefficient. The correlation between the two rankings was very strong ($R_s = 0.993$).

Table 2
Top-5 most critical combinations of single-, two-, three-, and four-link failures in the original Sioux Falls network.

Link combination	RO (USD)	Link combination	RO (USD)
(10,15)	73.2 % (0 %)	(10,15) (17,19) (18,20)	32.2 % (0 %)
(18,20)	74.0 % (0 %)	(9,10) (10,11) (18,20)	33.2 % (0 %)
(9,10)	75.3 % (0 %)	(10,15) (16,17) (18,20)	34.0 % (0 %)
(12,13)	77.7 % (0 %)	(5,9) (10,11) (10,15)	34.3 % (0 %)
(6,8)	77.8 % (0 %)	(9,10) (10,15) (18,20)	34.5 % (0 %)
(9,10) (10,11)	47.5 % (0 %)	(9,10) (10,11) (10,15) (18,20)	22.3 % (0 %)
(10,15) (18,20)	48.9 % (0 %)	(9,10) (10,11) (12,13) (18,20)	22.3 % (0 %)
(5,9) (10,11)	51.6 % (0 %)	(10,15) (10,17) (16,17) (18,20)	22.6 % (0 %)
(9,10) (18,20)	53.0 % (0 %)	(5,9) (10,11) (10,15) (15,19)	22.6 % (0 %)
(12,13) (18,20)	53.5 % (0 %)	(3,12) (9,10) (10,11) (18,20)	22.8 % (0 %)

RO = Network robustness indicator (Eq. 2); *USD* = Unsatisfied demand indicator (Eq. 3); Bold font = localised scenario.

3.5. Effect of demand variations on the network robustness and link criticality results

To evaluate the effect of demand variations on the aforementioned results, the analysis was repeated on versions of the Sioux Falls network with different demand distribution and intensity conditions (Section 2.4.3). For computational effectiveness, the disruption simulations were limited to single-, two- and three-link failures in these six case studies. The results are presented in Table 3, where the original Sioux Falls network is included for comparison. This table shows the mean and standard deviation of the flow/capacity ratio of the links in the network to provide a general measure of the congestion level. The low, medium, and high demand levels correspond to uncongested (mean flow/capacity ratio < 0.5), congested (mean flow/capacity ratio ≈ 1), and highly congested (mean flow/capacity ratio > 1.5) conditions, respectively.

The mean robustness indicator values of each network – computed over SLFs, 2LFs and 3LFs – was used as a general measure of the network robustness. The comparison of this value across the different case studies (Table 3) shows that higher demand and congestion reduce robustness. Furthermore, for the same congestion level, the networks where the demand was better distributed across the nodes were more robust.

To compare the impact of localised-, random-, and targeted-link failures in the case studies, the differences between the mean robustness indicator values in these three types of damage were computed (Table 3). The results suggest that the impact of localised and random failures were similar in all case studies (the absolute difference between the two means being inferior to 5%). Localised failures were more critical than random failures in some networks as the sign of the difference changed. However, this sign seemed correlated to neither the demand intensity nor the distribution. The difference between the impacts of targeted and random failures remained significant in all case studies ($\geqslant$7%). The differences were higher in the networks with concentrated demand (between 21.9% and 30.2%) than in the networks with distributed demand (between 7% and 21%).

Spearman's correlation coefficient was used to quantify the difference between the link criticality rankings derived from multiple- and single-link failures. The correlation coefficients (presented in Table 3) showed that the two rankings were always very strongly ($R_s \geqslant 0.80$) correlated. The correlation was stronger in the networks where the demand was distributed to all the nodes and increased further with the congestion level in both demand distribution cases.

The standard deviation of the link criticality values in each network was computed to evaluate the heterogeneity of the link criticality distributions in the networks. The results (presented in Table 3) showed that the heterogeneity was higher in the networks

Table 3

Effect of the demand distribution and intensity on the network initial state, robustness, and link-criticality.

	Demand concentrated in six nodes			Original Sioux Falls network	Demand distributed to all nodes		
Network initial state							
Demand level	Low	Medium	High	High	Low	Medium	High
Link flow/capacity ratio	0.40	1.08	2.19	1.47(0.57)	0.41	0.93	1.79
	(0.40)	(0.57)	(0.99)		(0.30)	(0.43)	(0.62)
Network robustness							
Mean robustness[1]	0.923	0.781	0.663	0.755	0.950	0.859	0.704
Difference between mean robustness to random and localised failures[2]	−0.006	−0.021	−0.033	0.022	0.001	−0.004	−0.012
Difference between mean robustness to random and targeted failures[2]	0.219	0.302	0.270	0.199	0.070	0.190	0.212
Link criticality							
SLF vs ALL[3]	0.971	0.991	0.998	0.993	0.994	0.996	0.998
Standard deviation of the link criticality values	0.083	0.168	0.191	0.108	0.026	0.078	0.142
Top-5 most critical links according to ALL (in criticality order)	(1,3)	(3,4)	(3,4)	(10,15)	(6,8)	(5,9)	(5,9)
	(6,8)	(1,3)	(3,12)	(18,20)	(12,13)	(3,4)	(3,12)
	(13,24)	(3,12)	(6,8)	(9,10)	(13,24)	(6,8)	(12,13)
	(12,13)	(4 5)	(4,5)	(12,13)	(1,3)	(1,3)	(13,24)
	(3,12)	(6,8)	(13,24)	(6,8)	(18,20)	(9,10)	(6,8)
Proportion of top-5 most critical 2LFs and 3LFs predicted by the iterative procedure	1.000	0.500	0.900	1.000	0.700	1.000	0.900
Run time[4]	4 min	25 min	56 min	33 min	2 min	8 min	2h41min

mean (standard deviation); [1] mean computed over single- (SLF), two- (2LF) and three- (3LF) link failures; [2] mean computed over 2LFs and 3LFs; [3] Correlation between the link criticality rankings based on single-(SLF) and multiple- (ALL) link-failures, ALL = SLF + 2LF + 3LF; [4]; Time taken to perform the SLF, 2LF and 3LF simulations using parallel processing on an *Intel i3-7100* 3.9 GHz and 8 GB memory work station.

with concentrated demand. Moreover, the heterogeneity of the link criticality distribution increased with the demand intensity in both demand distribution cases.

The top-5 most critical links in all case studies were identified based on SLFs, 2LFs and 3LFs using the criticality indicator. The lists of these critical links are presented in Table 3, where it can be seen that the criticality ranking depends on the demand distribution and intensity as all lists were different.

The accuracy of the iterative procedure proposed to identify and predict the impact of the top-5 most critical scenarios of MLFs (Section 3.3) was evaluated by computing the proportion of top-5 2LFs and 3LFs that could be predicted in the case studies (Table 3). This procedure was more accurate when the demand was distributed (the minimum proportion of scenarios identified was 50% when the demand was concentrated and 70% when it was distributed). This accuracy increased in congested networks (90–100% of the scenarios identified).

Fig. 6 shows the spatial distribution of link criticality values in the different demand intensity and distribution conditions. For the
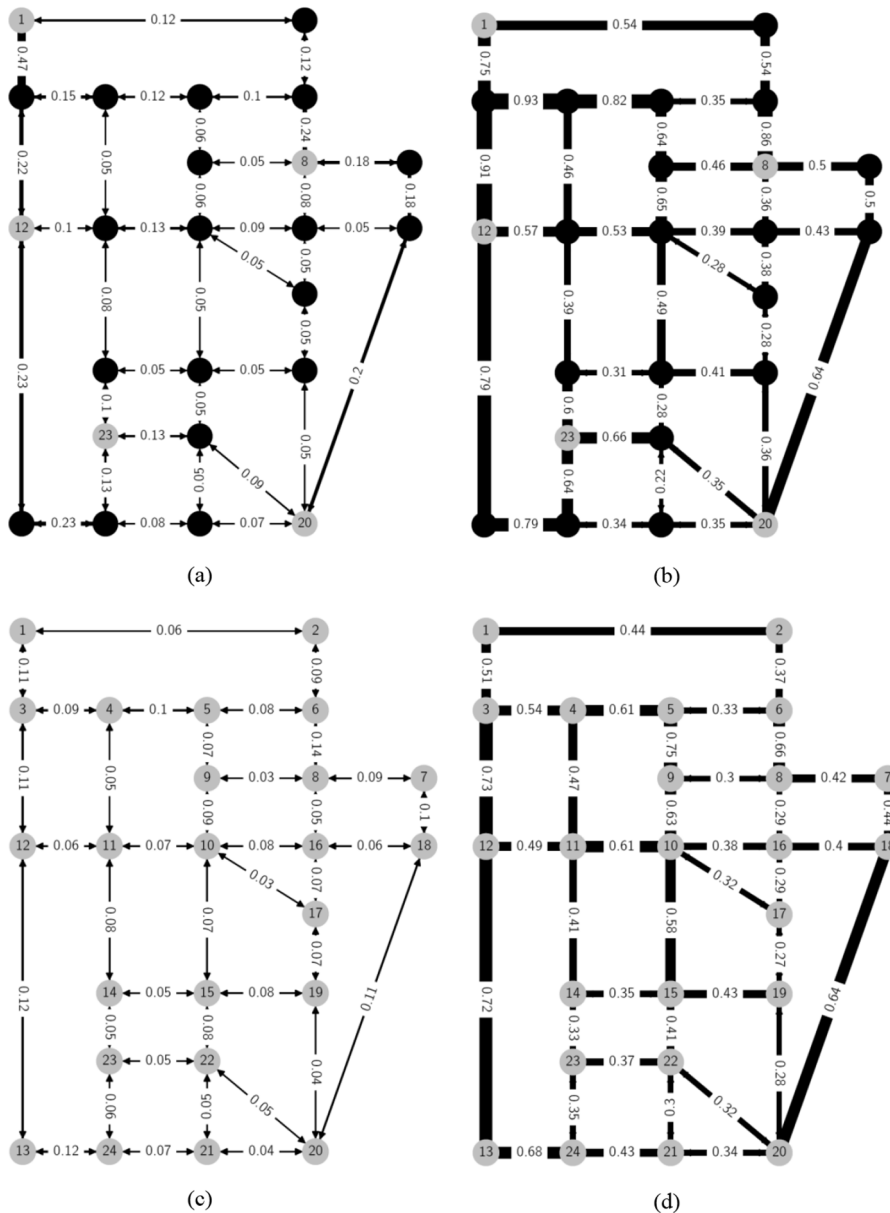

Fig. 6. Most critical links in the Sioux Falls network under different conditions: (a) low demand concentrated in six nodes, (b) high demand concentrated in six nodes, (c) low demand distributed to all nodes, and (d) high demand distributed to all nodes. The nodes in silver are OD points; the link labels and thickness indicate the values of the link criticality indicator, Cr_a, which combines the link criticality derived from single-, two-, and three-link failures into one indicator.

sake of brevity, only the low and high demand concentrated in six nodes and distributed across all nodes are shown. In Fig. 6, the link criticality values seem more heterogeneous in the networks with high and distributed demand, which is confirmed by the evolution of the standard deviation of the link criticality values in Table 3. Furthermore, it is interesting to note that in the uncongested networks (Fig. 6.a and c) the most critical links – (1,3), (6,8), (12,13) and (13,24) – were in the network periphery while in the congested networks (Fig. 6.b and d) some inner links – (4,5) and (5,9) – appeared among the top-5 most critical links (Table 4).

The correlation between the link criticality rankings derived in the different demand intensity and distribution conditions was evaluated (Table 4) to determine which ones were the closest to each other. Inside the demand distribution groups, the link criticality rankings were strongly correlated as the value of the correlation coefficient within the networks with concentrated and distributed demand remained above 0.767 and 0.698, respectively. Inside both groups, the correlation between the medium and high-level demand conditions increased further ($R_S > 0.90$). In contrast, the correlation between the rankings derived from the networks with concentrated and distributed demand was moderate to strong ($0.565 \leqslant R_s \leqslant 0.748$) and the correlation of the ranking in the original network with the other cases was moderate at best ($|R_S| \leqslant 0.575$).

4. Discussion

4.1. Measuring road network robustness

The comparison between the values derived from the network robustness indicator (measuring the demand-weighted average increase in travel time along the OD pairs) and the total *TT* change indicator showed conflicting results. The distributions of the total *TT* change indicator in the damage extension groups presented less pronounced peaks (Fig. 3.a), which suggests that this indicator provided a finer distinction between the impacts of the disruption scenarios than *RO*. As the ability to discriminate between the impacts of different scenarios – which helps towards the allocation of the limited resources to the most critical scenarios – is a desirable feature of robustness indices, *ToTTC* may appear to be better indicator.

However, the comparison also showed that contrary to *RO*, *ToTTC* provides a zero value for all disruption scenarios that lead to OD pairs disconnections despite the variability of the resulting unsatisfied demand. In Fig. 3.b, most of the scenarios causing OD pairs disconnections appear on the left side of the plots where *ToTTC* remains inferior to 10% while *RO* ranges between 12% and 95%. *ToTTC* is unable to discriminate between the impacts of scenarios causing OD pairs disconnections because these scenarios all result in very high total travel time values. This is because link unavailability is usually modelled by assigning a very high cost of travel to the damaged link such that when an OD pair is disconnected the travellers along this OD pair experience a very high and unrealistic travel cost. *RO* differentiates between the impacts of scenarios involving OD-pair disconnections because this indicator aggregates the values of the travel time change indices (TTC_w, Eq. 1) of all OD pairs, which include disconnected OD pairs with TTC_w values close to zero and non-disconnected OD pairs with higher TTC_w values.

Subsidiary indicators quantifying the spread of the impacts among the OD pairs and travellers can be used to complement the assessment including an indicator measuring the share of unsatisfied demand. The latter could even be combined with the conventional total *TT* increase index to provide an aggregated indicator able to consider the scenarios that lead to OD pair disconnections as proposed by Bagloee et al. (2017). However, as shown in Fig. 5.a and Table 2, several perturbation scenarios lead to the same proportion of unsatisfied demand. This would limit the ability of the aggregated indicator to discriminate between the impacts of these scenarios. In contrast, *RO* provides a single measure of the impacts and can discriminate between the impacts of most scenarios.

4.2. Network robustness and damage extension

The present study considered disruption scenarios concurrently affecting up to five links with the assumption that single-, two-, three-, four- and five-link failures could provide enough data points to understand the effect of the damage extension on the Sioux Falls network. The results partly validated this assumption. Single- to five-link failures allowed the evaluation of the effects of the two main mechanisms behind the loss of performance in disrupted networks: travel time increases and network (or OD pairs) disconnections. The later could be observed as certain two-link failures already fragmented the Sioux Falls network while some five-link failures led to larger disconnections. This is evidenced by the range of the maximum value of the unsatisfied demand indicator (*USD*) that increased from 0% in 1LFs to 15% in 5LFs. As this indicator mainly depends on the network connectivity, it is comparable to the network

Table 4

Correlation (R_S) between the link criticality rankings derived in different demand intensity and distribution conditions.

	Demand level	Demand concentrated in six nodes			Demand distributed to all nodes		
		Low	Medium	High	Low	Medium	High
Demand concentrated in six nodes	Low						
	Medium	0.824					
	High	0.767	0.948				
Demand distributed to all nodes	Low	0.663	0.618	0.565			
	Medium	0.565	0.718	0.703	0.777		
	High	0.610	0.753	0.748	0.698	0.918	
Original Sioux Falls network	High	0.113	0.225	0.267	0.507	0.575	0.532

robustness indicators used in certain topological studies measuring road network robustness by the reduction in the size of the giant (or largest connected) component of the network under dismantling processes (Casali and Heinimann, 2020; Buhl et al., 2006). The data points obtained for the maximum values of *USD* (Fig. 4.b) are consistent with the first points of the plots shown in these studies. In the later, the size of the giant components under targeted dismantling processes decreases in two – for small networks composed of few hundred nodes in Buhl et al. (2006) – or three – for large networks composed of thousands of nodes in Casali and Heinimann (2020) – main stages. In small networks, the most detrimental stage to the network performance (or transition phase) occurs in the first stage (when 0–30% of the links are disrupted) while in large networks the transition occurs in the second stage (when 10–40% of the links are disrupted). The Sioux Falls network being small, the transition phase started with 2LFs and it can be expected that the maximum value of *USD* will continue to rapidly increase reaching a value of approximately 90% when up to 30% of the links ($\approx$ 11 links in the Sioux Falls network) will be disrupted as reported in Buhl et al. (2006).

However, the present results also showed that certain five-link failures (that disrupt 13% of links in the Sioux Falls network) can cause 87.4% decreases in network performance measured by the demand-weighted average increase in travel time along the OD pairs (*RO*) as shown in Fig. 4.a. This value means that the travel time of most travellers would be multiplied by eight. Therefore, single- to five-link failures provided sufficient data points to understand the full range of potential impacts caused by multiple-link failures on the travel time in the Sioux Falls network. Besides, the present results showed that the evolution of the mean and minimum robustness indicator values with respect to the damage extension could be represented by linear and piecewise linear models, respectively (Fig. 4. a). The extra data points could hence be predicted using these models.

Ultimately, the present results show that the same disruption scenario can lead to major consequences in terms of travel time increases but minor consequences in terms of network (or OD pairs) disconnections. This shows that topological studies, which disregard traffic flows and potential congestion to focus on the network structure can overestimate the robustness of road networks.

4.3. Impact of random, localised and targeted damage

The comparison of the impacts of the three types of damage in the original Sioux Falls network (Table 2 and Fig. 5) showed that the most critical types of scenarios were in this order: targeted, localised, and random failures; and that targeted attacks were significantly more detrimental to the network performance than random failures (20% difference) while localised failures were only slightly more critical than random failures (3% difference in average). These results are consistent with the findings of Hu et al. (2016) that however considered full dismantling processes rather than failure scenarios disrupting a limited number of roads.

Furthermore, the comparison of the difference between the mean robustness in localised and random failures across different demand intensity and distribution conditions (Table 3) showed that their impacts were very close (the mean difference being inferior to 5%) and that one could be slightly more detrimental than the other in different conditions. This suggests that although random scenarios damage infrastructures distributed throughout the whole network (and therefore potentially impact more users) the resulting impact is in general equivalent to the impact of localised failures. Hence, the impact may be significant in one of the locations disturbed only.

The analysis of the unsatisfied demand resulting from the different types of damage (Fig. 5) showed that localised failures lead to higher proportions of unsatisfied demand than their targeted counterparts. Hence, localised damage cause a maximum impact to a limited number of road users. In contrast, targeted attacks strategically damage network components that are apart (as shown in Table 2 where the top-5 most critical combinations of link failures rarely involved adjacent links) but whose simultaneous failures cause important and widespread impacts (the mean difference between the impact of targeted and random failures remained superior to 7% in robustness in all case studies in 3). The difference was greater in the networks where the demand was concentrated in a few nodes compared to networks where the demand was distributed to all nodes. This is because in the former it is easier to cause important and widespread impacts with limited resources (number of disrupted links) as more vehicles share the same routes. This explanation is confirmed by the relatively high heterogeneity of the link criticality values observed in the networks with concentrated demand compared to the other cases (Table 3). In contrast, in the networks with distributed demand, most links tend to be equally critical, which explains why the extended impact of targeted attacks (i.e. the difference between the impact of targeted and random damage) is reduced when the demand is well distributed.

The demand intensity has a similar impact on the network as the heterogeneity of the link criticality values, as well as, the extended impact of targeted attacks increased with the demand intensity for both demand distribution conditions (except that in the concentrated demand condition the extended impact of targeted attacks was higher with the medium demand than with the high demand). Therefore, it is more crucial to identify and protect the most critical links in networks that are congested and where the demand is not well distributed among the intersections.

4.4. Identification and sensitivity of the most critical scenarios and links

4.4.1. Predictability of scenarios' and links' criticality rankings

Wang et al. (2016) showed that the links involved in the most critical multiple-link failures are not simply the combination of the most critical links with single-link failure. The present results went further to show that the most critical links and scenarios are not completely random. The top-5 most critical scenarios of different sizes (i.e. SLFs, 2LFs, etc.) were related to each other as the top-5 most critical scenarios of size M tented to appear in the top-5 most critical scenarios of size $M + 1$. This led to an iterative procedure (described in Section 3.3) providing a heuristic to identify and predict the impact of these scenarios with a decreased computational effort.

This pattern and therefore the accuracy of the procedure seemed stronger and higher, respectively, in congested networks. This may be because all links are used in congested networks since road users along the same OD pairs use several routes to minimise their respective travel times. Therefore, in congested networks there is a limited spare capacity available to accommodate the users that need to re-route following a disruption such that disruptions mainly lead to additional congestion. The most critical scenarios of size M are hence likely to appear in the most critical scenarios of size $M + 1$. Whereas in uncongested networks, travellers along the same OD pairs tend to use the same route such that some links may be unused and provide a good alternative for re-routing when disruptions occur, leading to limited network performance losses. Hence, the combined effect of the link failures seems more difficult to predict in uncongested networks.

For the same reason, the proposed procedure can also provide a satisfying approximation of the link criticality ranking in congested networks as this procedure requires the computation of all SLFs, which according to the present results were very strongly correlated to the rankings based on MLFs in congested networks ($R_S > 0.990$). These results complement the findings of Sohouenou et al. (2020) that show the influence of the network size, topology, and demand distribution on the correlation between SLF- and MLF-based criticality rankings but do not consider the influence of congestion.

The limited accuracy of the iterative procedure in uncongested networks is not bad news considering that traffic simulations are less computationally expensive in uncongested networks than in congested networks as shown by the run times reported in Table 3. This is because the user equilibrium is easier to compute in uncongested networks. Indeed, the FW algorithm seeks to find the equilibrium traffic flows where the travel time of each traveller is minimum. To this end, the algorithm incrementally assigns the OD demand in multiple steps such that in each step a fraction of the OD matrix is loaded to the shortest paths and the resulting link travel time calculated (depending on the link flow). The re-calculated link travel times are used in the following step to find new shortest paths for the OD pairs. In uncongested networks, the equilibrium search is rapid as the link travel times are independent of link flows such that most travellers along an OD pair use the same route. Whereas in congested networks, travellers along an OD pair use several routes to reduce their travel time as congestion builds up, leading to a greater number of iterations required to reach the equilibrium.

Finally, it is interesting to note that the pattern found between the top-5 most critical link combinations suggests that, in practice, the protection or rapid repair of the top-5 most critical links with SLF can also help towards the protection of the network performance against the most critical MLF scenarios as the latter tend to involve at least one of the top-5 most critical links with SLF.

4.4.2. Influence of the demand intensity and distribution on the link criticality rankings

The results showed that the link criticality rankings are sensitive to the demand intensity and distribution (Tables 3 and 4). The significant difference observed between the criticality rankings in the demand distribution conditions considered (demand heterogeneously distributed in the original Sioux Falls network, concentrated in six nodes, and homogeneously distributed to all nodes) was expected since the demand distribution modifies the network usage. The difference observed between the demand intensity (low, medium, and high) conditions was more interesting. The very strong correlation found between the medium and high demand conditions regardless of the demand distribution (Table 4) showed that the links' ranking significantly changes as the network moves from uncongested to congested conditions but remains similar when congestion further increases.

In addition, the analysis of the spatial distribution of the link criticality values in the network (Fig. 6) showed that the main difference between the uncongested and congested conditions was the fact that in the former the most critical links belonged to the network periphery while some inner links appeared among the top-5 most critical links in the congested networks. In uncongested networks, when an inner link is unavailable the network structure naturally provides several alternatives routes that lead to reasonable increases in travel time for the affected users, whereas, in congested networks, these alternative routes are already jammed and therefore lead to greater TT increases.

To conclude, this shows that the accuracy of the demand distribution model is important for robustness assessments as this will significantly impact the resulting link criticality rankings. In contrast, the accuracy of the demand intensity evaluation seems less crucial if the network is accurately defined as uncongested or congested in its undisrupted state. Hence, practitioners should carefully think about the conditions that they wish to consider when performing road network robustness assessments. They may, for example, choose to consider the peak-hour conditions that should represent the worst-case scenarios in terms of demand intensity; or prioritise the demand going from/to critical locations (for example hospitals, fire stations and airports) that may lead to a different demand distribution than the dominant peak-hour home-work trips; or consider and combine both. This sensitivity analysis also provides some insights into the potential effect of the travel demand alteration caused by disruptions on the present assessment. Following a major disruption, work and leisure trips are likely to be cancelled or delayed while emergency trips (e.g. evacuation and transport from/to hospitals) are likely to increase. Hence, the travel demand is likely to concentrate in a few zones while the total demand intensity decreases. The low- and medium-demand intensity concentrated in six nodes may represent such conditions in the Sioux Falls network. In these conditions, the network robustness increased and the link criticality rankings completely changed (Table 3).

5. Conclusions

In line with the hazard-independent approach suggested by the resilience paradigm, this paper investigated the impact of all scenarios concurrently disrupting up to five links in the Sioux Falls network. This represents over five hundred thousand disruption scenarios across the different demand intensity and distribution conditions considered. This approach allows understanding the potential impact of a wide range of disruptive events, including unpredictable events that could be overlooked by risk analyses focusing on a few predictable scenarios. This study led to five key conclusions:

- The widely adopted robustness-quantification approach that measures network robustness by the total travel-time losses cannot discriminate between the impacts of the scenarios disconnecting OD pairs. The discrimination between these scenarios remains important as they are manifold and lead to different proportions of stranded road users. Hence, this discrimination could help transport practitioners and public authorities in the allocation of the limited resources available for road infrastructures construction and maintenance to the most critical scenarios and links.
- To discriminate between the impacts of scenarios that lead to OD-pair disconnections, it is necessary to consider the impacts on the OD pairs (or users) separately rather than the total travel-time losses in the network. This can be achieved by measuring the relative change of the travel time along the OD pairs. The proposed robustness indicator uses a demand-weighted average to aggregate these relative change values into one indicator.
- The demand distribution (i.e. how the demand for travel, or population, is distributed among the network intersections) and intensity (i.e. whether the network is congested in the undisrupted state) significantly influence the robustness assessment results especially the link criticality rankings. Hence, practitioners need to carefully consider the traffic conditions for which the resilience assessment is made and also the possible evolution of these traffic conditions.
- Random and localised damage (disrupting the same number of links) generally lead to similar consequences while intentional attacks target links that may be apart or not critical on their own but whose combined disruptions create a maximised and widespread impact. Besides, targeted attacks are even more detrimental to the network performance in comparison to random failures when the demand for travel (or population) is high and concentrated among a few nodes.
- In congested networks, it may not be necessary to simulate all possible disruption scenarios to identify and assess the impact of the most critical scenarios of multiple-link failures. Instead, a procedure that requires the computation of all SLF scenarios, followed by the computation of the top-10 most critical scenarios of 2LFs, 3LFs, etc. can be used. In uncongested networks, the proposed procedure may not provide satisfactory results. However, the lower computational time of the traffic simulations in uncongested networks reduces the need for such a procedure as the full-scan approach that simulates all possible scenarios of multiple-link failures may be used in this case.

The full-scan approach adopted in this study is limited by computational capacity. Its application is currently realistic for small to medium (sub) network models composed of up to a few hundred links only. The removal of residential and service roads (that are not designed for through movements) as well as intersections connecting one to two links from network models, which have a minor impact on the estimated travel speeds as shown in Ganin et al. (2017), may help to reach this threshold in certain cases. Alternatively, further optimisation of the traffic assignment algorithm and high-performance computing may help to increase this threshold. Future works could investigate the scalability of this approach to validate the applicability of the present findings to large networks. This may lead to the development of frameworks for assessing road network robustness under multiple disruption scenarios, which rely on heuristics (such as the proposed iterative procedure for identifying the most critical scenarios) that decrease the computational burden of the assessment.

Disclaimer

The views expressed are purely those of the authors and may not in any circumstances be regarded as stating an official position of the European Commission.

Acknowledgements

References

Alderson, D.L., Brown, G.G., Carlyle, W.M., Wood, R.K., 2017. Assessing and Improving the Operational Resilience ol a Large Highway Infrastructure System to Worst-Case Losses. Transp. Sci. 52 (4), 1012–1034. https://doi.org/10.1287/trsc.2017.0749.

ARUP, 2014. City Resilience Framework (tech. rep.). Arup. London, UK. https://www.preparecenter.org/sites/default/files/arup%7B%5C_%7Drockefeller%7B%5C_%7Dresilient%7B%5C_%7Dcities%7B%5C_%7Dreport.pdf.

Bagloee, S.A., Sarvi, M., Wolshon, B., Dixit, V., 2017. Identifying critical disruption scenarios and a global robustness index tailored to real life road networks. Transp. Res. Part E: Logist. Transp. Rev. 98, 60–81. https://doi.org/10.1016/j.tre. 2016.12.003.

Bhavathrathan, B.K., Patil, G.R., 2015. Quantifying resilience using a unique critical cost on road networks subject to recurring capacity disruptions. Transp. A: Transp. Sci. 11 (9), 836–855. https://doi.org/10.1080/23249935.2015.1087230.

Bhavathrathan, B.K., Patil, G.R., 2018. Algorithm to Compute Urban Road Network Resilience. Transp. Res. Rec. 2672 (48), 104–115. https://doi.org/10.1177/0361198118793329.

Boyce, D., Ralevic-Dekic, B., Bar-Gera, H., 2004. Convergence of traffic assignments: How much is enough? J. Transp. Eng. 130 (1), 49–55. https://doi.org/10.1061/(ASCE)0733-947X(2004)130:l(49).

Buhl, J., Gautrais, J., Reeves, N., Sole, R.V., Valverde, S., Kuntz, P., Theraulaz, G., 2006. Topological patterns in street networks of self-organized urban settlements. Eur. Phys. J. B 49 (4), 513–522. https://doi.org/10.1140/epjb/e2006-00085-l.

Bureau of Public Roads, 1964. Traffic Assignment Manual: Bureau of Public Roads (tech. rep.). U.S. Department of Commerce, Washington, D.C.

Casali, Y., Heinimann, H.R., 2019. A topological characterization of flooding impacts on the Zurich road network. PLoS ONE 14 (7). https://doi.org/10.1371/journal.pone.0220338.

Casali, Y., Heinimann, H.R., 2020. Robustness response of the Zurich road network under different disruption processes. Comput. Environ. Urban Syst. 81 (101460) https://doi.org/10.1016/j.compenvurbsys.2020.101460.

Demirel, H., Kompil, M., Nemry, F., 2015. A framework to analyze the vulnerability of European road networks due to Sea-Level Rise (SLR) and sea storm surges. Transp. Res. Part A: Policy Pract. 81, 62–76. https://doi.org/10.1016/j.tra.2015.05.002.

D'Lima, M., Medda, F., 2015. A new measure of resilience: An application to the London Underground. Transp. Res. Part A: Policy Pract. 81, 35–46. https://doi.org/10.1016/j.tra.2015.05.017.

Ganin, A.A., Kitsak, M., Marchese, D., Keisler, J.M., Seager, T., Linkov, I., 2017. Resilience and efficiency in transportation networks. Sci. Adv. 5 (12), el701079. https://doi.org/10.1126/sciadv.l701079.

Hu, F., Yeung, C.H., Yang, S., Wang, W., Zeng, A., 2016. Recovery of infrastructure networks after localised attacks. Sci. Rep. 6 (24522) https://doi.org/10.1038/srep24522.

LeBlanc, L.J., Morlok, E.K., Pierskalla, W.P., 1975. An efficient approach to solving the road network equilibrium traffic assignment problem. Transp. Res. 9 (5), 309–318. https://doi.org/10.1016/0041-1647(75)90030-1.

Mattsson, L.G., Jenelius, E., 2015. Vulnerability and resilience of transport systems – A discussion of recent research. Transp. Res. Part A: Policy Pract. 81, 16–34. https://doi.org/10.1016/j.tra.2015.06.002.

Mitradjieva, M., Lindberg, P.O., 2013. The Stiff Is Moving - Conjugate Direction Frank-Wolfe Methods with Applications to Traffic Assignment. Transp. Sci. 7 (2), 280–293.

Nogal, M., O'Connor, A., Caulfleld, B., Martinez-Pastor, B., 2016. Resilience of traffic networks: From perturbation to recovery via a dynamic restricted equilibrium model. Reliab. Eng. Syst. Saf. 156, 84–96. https://doi.org/10.1016/j.ress.2016.07.020.

Omer, M., Mostashari, A., Nilchiani, R., 2013. Assessing resilience in a regional road-based transportation network. Int. J. Ind. Syst. Eng. 13 (4), 389–408. https://doi.org/10.1504/IJISE.2013.052605.

Ortuzar, J.D.D., Willusem, L.G.. 2011. Modelling Transport, fourth ed., Oxford, Wiley. https://doi.org/10.1002/9781119993308.

Park, J., Seager, T.P., Rao, P.S., Convertino, M., Linkov, I., 2013. Integrating risk and resilience approaches to catastrophe management in engineering systems. Risk Anal. 33 (3), 356–367. https://doi.org/10.1111/j.l539-6924.2012.01885.x.

Puth, M.T., Neuhauser, M., Ruxton, G.D., 2015. Effective use of Spearman's and Kendall's correlation coefficients for association between two measured traits. Anim. Behav. 102, 77–84. https://doi.org/10.1016/j.anbehav.2015.01.010.

Reka, A., Hawoong, J., Barabasi, A.-L., 2000. Error and attack tolerance of complex networks. Nature 406, 378–382.

Sohouenou, P.Y.R., Christidis, P., Christodoulou, A., Neves, L.A.C., Lo Presti, D., 2020. Using a random road graph model to understand road networks robustness to link failures. Int. J. Crit. Infrastruct. Prot. https://doi.org/10.1016/j.ijcip.2020.100353.

Sohouenou, P.Y.R., Neves, L.A.C., Lo Presti, D., 2019. Resilience indicators for road networks: the role of robustness and rapidity. In: 2019 international conference on smart cities (icsc), Seoul, South Korea. https://nottingham-repository.worktribe.com/output/2546559.

Sullivan, J.L., Novak, D.C., Aultman-Hall, L., Scott, D.M., 2010. Identifying critical road segments and measuring system-wide robustness in transportation networks with isolating links: A link-based capacity-reduction approach. Transp. Res. Part A: Policy Pract. 44 (5), 323–336. https://doi.org/10.1016/j.tra.2010.02.003.

Taylor, M.A., Sekhar, S.V., D'Este, G.M., 2006. Application of accessibility based methods for vulnerability analysis of strategic road networks. Netw. Spatial Econ. 6, 267–291. https://doi.org/10.1007/sll067-006-9284-9.

Transportation Networks for Research Core Team, 2019. Transportation Networks for Research. Retrieved December 8, 2019, from. https://github.com/bstabler/TransportationNetworks.

Wang, D.Z.W., Liu, H., Szeto, W.Y., Chow, A.H.F., 2016. Identification of critical combination of vulnerable links in transportation networks - a global optimisation approach. Transportmetnca A: Transp. Sci. 12 (4), 346–365. https://doi.org/10.1080/23249935.2015.1137373.

Wisetjindawat, W., Kermanshah, A., Derrible, S., Fujita, M., 2017. Stochastic Modeling of Road System Performance during Multihazard Events: Flash Floods and Earthquakes. J. Infrastruct. Syst. 23 (4), 04017031. https://doi.org/10.1061/(asce)is.1943-555x.0000391.

Xie, F., Levinson, D., 2011. Evaluating the effects of the I-35W bridge collapse on road-users in the twin cities metropolitan region. Transp. Plan. Technol. 34 (7), 691–703. https://doi.org/10.1080/03081060.2011.602850.

Zanin, M., Sun, X., Wandelt, S., 2018. Studying the Topology of Transportation Systems through Complex Networks: Handle with Care. J. Adv. Transp. 2018 https://doi.org/10.1155/2018/3156137.

Zhang, W., Wang, N., 2016. Resilience-based risk mitigation for road networks. Struct. Saf. 62, 57–65. https://doi.org/10.1016/j.strusafe.2016.06.003.

Zhou, Y., Sheu, J.-B., Wang, J., 2017. Robustness Assessment of Urban Road Network with Consideration of Multiple Hazard Events. Risk Anal. 37 (8), 1477–1494. https://doi.org/10.1111/risa.l2802.